EUKARYOTIC CELL, Aug. 2005, p. 1493–1502 Vol. 4, No. 8
1535-9778/05/$08.00+0 doi:10.1128/EC.4.8.1493–1502.2005

Candida albicans Biofilm-Defective Mutants

Mathias L. Richard,[1]† Clarissa J. Nobile,[1,2] Vincent M. Bruno,[1,3] and Aaron P. Mitchell[1]*

Department of Microbiology, Columbia University, New York, New York 10032[1]; Biological Sciences Program, Department of Biological Sciences, Columbia University, New York, New York 10027[2]; and Program in Cellular, Molecular, and Biophysical Studies, Columbia University, New York, New York 10032[3]

Received 4 June 2004/Accepted 17 June 2005

Biofilm formation plays a key role in the life cycles and subsistence of many microorganisms. For the human fungal pathogen *Candida albicans*, biofilm development is arguably a virulence trait, because medical implants that serve as biofilm substrates are significant risk factors for infection. The development of *C. albicans* biofilms in vitro proceeds through an early phase, in which yeast cells populate a substrate, an intermediate phase, in which pseudohyphal and hyphal cell types are produced, and a maturation phase, in which continued cell growth is accompanied by accumulation of an extracellular matrix. Here we report the results of a screen for *C. albicans* biofilm-defective mutants, in which homozygous insertions in *NUP85*, *MDS3*, *KEM1*, and *SUV3* were found to block biofilm development. Confocal microscopic examination suggests that *nup85*, *suv3*, and *mds3* mutations cause early-phase arrest, whereas the *kem1* mutation causes intermediate-phase arrest. All of the mutants are defective in hypha production in several media. Analysis of mixed-biofilm development indicates that all of the mutants are defective in the production of hyphae in the context of a biofilm. Because all of the mutants are defective in the retention of cells in the biofilm, we infer that hyphae provide an adherent scaffold that stabilizes the biofilm structure.

Microorganisms are often studied as a mass of cells suspended in a liquid medium, but in nature these organisms routinely interact with surfaces. There are two general types of cell-surface interaction: population and penetration. Population is the phenomenon of surface colonization to produce a biofilm (9, 50); penetration is the phenomenon of surface invasion (5, 14, 27, 38, 46, 52). Both interactions often involve differentiation, as illustrated by the unique phenotypes manifested by biofilm cells and the specific structures, such as hyphae and appressoria, that are elaborated for surface disruption. The interactions are not mutually exclusive, and surfaces may be modified during biofilm development to facilitate invasion.

The human fungal pathogen *Candida albicans* can populate and penetrate surfaces. The ability to penetrate a surface has long been appreciated as a key virulence trait (14, 38), because the commensal *C. albicans* cells of mucosal and intestinal surfaces can serve as the source for invasive infection (45, 53). However, the ability of *C. albicans* to populate a surface and produce a biofilm is also a virulence trait (9, 29). Medical implants such as vascular catheters are significant risk factors for *C. albicans* infection, and biofilms have been observed on device surfaces after removal from patients (29). Indeed, one form of *Candida* infection, called thrush or oropharyngeal candidiasis, is a dense fungal mat adhering to the oral mucosal surface. Therefore, thrush may be considered an infecting biofilm. Thus, the ability of *C. albicans* to form a biofilm has a profound impact on its ability to cause disease.

Biofilms of *C. albicans* have been characterized in considerable detail. They are composed of a mixture of cell types, including yeast, pseudohyphal, and hyphal cells, and include an extracellular matrix comprising polysaccharide and protein (9, 31). Like bacterial biofilms, *C. albicans* biofilms are much more resistant than free-living planktonic cells to many antimicrobial drugs (18, 42, 43). This biofilm-specific cell property provides a very clear link to virulence and has prompted much recent interest in *C. albicans* biofilm structure, physiology, and regulation.

C. albicans biofilm development occurs in three phases, as observed with in vitro models (4, 9). During the early phase, yeast cells adhere to the surface of the support and begin to divide and form a layer of microcolonies. During the intermediate phase, continued yeast cell growth is accompanied by extracellular material production and initial differentiation to produce elongated pseudohyphae and hyphae. Finally, a maturation phase occurs, in which the amount of extracellular material increases, and the network of pseudohyphae and hyphae embedded in this matrix grows in parallel to assemble a biofilm of at least 200 μm in depth. The precise kinetics and sequence of events depend upon the substrate and biofilm growth medium (4, 17, 42), as well as the *C. albicans* strain (22, 33, 47).

A few genes that govern biofilm formation have been characterized. Ramage et al. have shown that the hyphal regulatory gene *EFG1* is required for normal biofilm growth (1, 44). Reduced hypha production by the *efg1*/*efg1* mutant and the more extreme *efg1*/*efg1 cph1*/*cph1* mutant (34, 36) certainly contributes to the biofilm defect, but the mutants also appeared to adhere poorly to the substrate (1, 44). Similarly, the presence of the quorum-sensing molecule farnesol, an inhibi-

* Corresponding author. Mailing address: Department of Microbiology, Columbia University, Hammer Building, Room no. 906, 701 West 168th Street, New York, NY 10032. Phone: (212) 305-8251. Fax: (212) 342-4070. E-mail: apm4@columbia.edu.

† Present address: Laboratoire de Microbiologie et Génétique Moléculaire, INA P-G, UMR-INRA216, URA-CNRS1925, BP01, 78850 Thiverval-Grignon, France.

tor of hypha formation, inhibits biofilm formation (30). The general amino acid control regulatory gene *GCN4* is also required for full biofilm biomass production, though the *gcn4*/*gcn4* mutant does not display a qualitative developmental defect (11). *GCN4* is required for hypha formation under some growth conditions (51) but apparently not in the context of a biofilm. Finally, a contact-activated protein kinase, Mkc1p, is required for biofilm development (32), thus suggesting that *C. albicans* may respond uniquely to surface contact during biofilm formation.

The understanding of bacterial biofilms has advanced enormously in recent years (6, 16, 41). A substantial contribution to this understanding has come from the identification and analysis of biofilm-defective mutants. Such studies have defined roles for adherence, motility, and extracellular matrix materials in bacterial biofilm development (6, 41). We describe here the results of a screen for *C. albicans* mutants defective in biofilm formation. Genetic characterization of random mutants has been a challenge with this organism because it is an asexual diploid. However, the *C. albicans* genomic sequence has provided a platform for molecular gene disruption technologies that cause partial or complete gene function defects (2). Here we used a collection of insertion mutations in 197 different open reading frames (ORF) (3, 8, 40) to identify biofilm-defective mutants. Our results permit the genetic definition of two different blocks in biofilm development, which (as we discuss) might correspond to two temporal stages in the development of wild-type biofilms. Analysis of mixed biofilms comprising both wild-type and mutant cells indicates that the mutants described here have defects in hypha formation in the context of a biofilm.

MATERIALS AND METHODS

Yeast strains and media. All *C. albicans* strains (Table 1) were derivatives of strain BWP17 (genotype, *ura3*::λ*imm434*/*ura3*::λ*imm434 arg4*::*hisG*/*arg4*::*hisG his1*::*hisG*/*his1*::*hisG* [54]). The His$^-$ homozygous insertion mutant strains, created in this lab by random transposon mutagenesis with the *UAU1* cassette, have been described previously (8). We used two different reference strains (Table 1) for comparison to mutants. DAY286 is an Arg$^+$ Ura$^+$ His$^-$ derivative of strain BWP17 and was used for comparison to Arg$^+$ Ura$^+$ His$^-$ mutant strains. DAY185 is an Arg$^+$ Ura$^+$ His$^+$ derivative of strain BWP17 and was used for comparison to Arg$^+$ Ura$^+$ His$^+$ mutant strains.

C. albicans strains were grown in yeast extract-peptone-dextrose plus uridine (2% dextrose, 2% Bacto peptone, 1% yeast extract, and 80 μg/ml uridine) at 30°C. Following transformation, selection was accomplished on synthetic medium (2% dextrose, 6.7% yeast nitrogen base plus ammonium sulfate, and the necessary auxotrophic supplements).

These media followed standard recipes (7). Biofilms were cultured in SD medium plus 50 mM glucose (50 mM dextrose, 6.7% yeast nitrogen base plus ammonium sulfate, and the necessary auxotrophic supplements [17]) or, when noted, in Spider medium (1% Difco nutrient broth, 1% mannitol, 0.2% dibasic potassium phosphate, and auxotrophic supplements if necessary [35]).

Biofilm growth. Squares of silicone (1.5 cm by 1.5 cm) were cut from silicone sheets (Cardiovascular Instrument Corp.), washed in water, and autoclaved. Prior to inoculation, the squares were incubated with bovine serum (B-9433; Sigma) overnight and then washed once in phosphate-buffered saline (PBS) immediately before inoculation. Strains were grown overnight in yeast extract-peptone-dextrose at 37°C and diluted in SD medium plus 50 mM glucose to an optical density at 600 nm (OD_{600}) of 1.0 or in Spider medium to an OD_{600} of 0.5. Inoculation was accomplished by adding 2 ml of this cell suspension to a silicone square in a 12-well plate and incubating at 37°C for 90 min with gentle agitation (~150 rpm). After this adherence step, each square was washed with PBS and 2 ml of fresh medium was added. Biofilms were grown for 60 h at 37°C with gentle agitation.

For the mutant screen, two independent isolates of each insertion mutant were tested. For biomass dry mass determinations, each biofilm was removed from the substrate by vortexing the silicone square in PBS and then filtering the cell suspension on preweighed filter paper. The filtrate and filter were dried at 75°C overnight and then weighed. The average dry biomass was calculated from six independent samples.

Reconstitution of wild-type alleles. The ORF affected by each insertion was identified through sequence determination and BLASTN searches (8) to the *Candida albicans* genome database (http://www-sequence.stanford.edu/group/candida/). Insertion sites were localized to codon 572 out of 774 for *nup85*::Tn*7*, codon 81 out of 686 for *mds3*::Tn*7*, codon 770 out of 1,469 for *kem1*::Tn*7*, and codon 365 out of 720 for *suv3*::Tn*7*.

The construction of reconstituted strains for *SUV3* (orf19.4519) and *MDS3* (orf19.6759) has been described previously (8, 40). Reconstituting the *NUP85* (orf19.5887) and *KEM1* (orf19.4969) plasmids was done as follows. PCR was used to produce a fragment for *NUP85* from approximately 1,000 bp upstream of the ATG to approximately 300 bp downstream of the stop codon of the *NUP85* ORF. Because of the size of the *KEM1* ORF, the strategy used was to integrate the complementing plasmid at the *KEM1* locus by using a PCR fragment of a part of the *KEM1* ORF and thus reconstitute a functional *KEM1* allele. The PCR product for *KEM1* begins 600 bp upstream of the site of integration (BstEII restriction site) and ends 250 bp downstream of the stop codon. *NUP85* and *KEM1* PCR fragments were inserted into the pGEMT-Easy vector (Promega), which contains NotI sites flanking the insertion. The inserts were released through NotI digestion and ligated into NotI-digested dephosphorylated pDDB78, a *HIS1* vector (49), to generate plasmids pMLR2 (containing the *NUP85* insert) and pMLR8 (containing the *KEM1* insert). Strain MLR12 was constructed by transforming GKO814, the *nup85*/*nup85* homozygous insertion mutant, with the NruI-digested plasmid pMLR2 to histidine prototrophy. The unique NruI site in this plasmid lies in *HIS1* sequences, and NruI digestion thus directs integration to the *HIS1* locus. Strain MLR28 was constructed by transforming GKO798, the *kem1*/*kem1* homozygous insertion mutant, with the BstEII-digested plasmid pMLR8 to histidine prototrophy, directing the integration to the *KEM1* locus.

GFP expression in mutant and reference strains. The green fluorescent protein (GFP) ORF and *ADH1* terminator were amplified by PCR with pGFP-HIS1 as a template (12). Primers were designed to add EcoRI and SpeI restriction sites upstream and downstream, respectively, of the GFP gene. The fragment was ligated to EcoRI- and SpeI-digested vector pTEF1 to yield plasmid pMLR31. pTEF1 is a vector derived from plasmid pDDB78 (49) that harbors the strong *C. albicans TEF1* promoter. A unique NruI site in this plasmid lies in *HIS1* sequences, and NruI digestion thus directs integration to the *HIS1* locus. Each His$^-$ insertion mutant strain was transformed with NruI-digested pMLR31 to produce a strain that expresses GFP.

***KEM1* deletion construction.** We created *kem1*Δ::*ARG4* and *kem1*Δ::*URA3* DNA fragments by PCR product-directed gene deletion (54), using 80-mer oligonucleotides kem1-3DR (5′-CAATAATGCATTACTGATAACTGTAAGAGAATGGAATATCTGACATATTCATATGGGTGGAATTGTGAGCGGATA) and kem1-5DR (5′-GAGATAGACATATATCATGGGTATGTTATTTGTTGTTAGATTCTGCTAAATCCCTAGTGTTTCCCAGTCACGACGTT). The *kem1*Δ/*kem1*Δ mutant, strain MLR74, was derived from strain BWP17 through two successive transformations and lacks the entire *KEM1* ORF.

CSLM images. Confocal scanning laser microscopy (CSLM) images were obtained in the Columbia University Optical Microscopy Facility by using a Zeiss LSM510 NLO multiphoton confocal microscope. This system is composed of a Zeiss Axioskop 2 FS MOT upright microscope and a laser with multiphoton capability. Biofilms were stained in a 2-ml solution with either 0.2 mg/ml calcofluor white (fluorescent brightener 28, F3543; Sigma) or 50 to 100 μg/ml Alexa conjugate of concanavalin A (Alexa Fluor 594 nm, C-11253; Molecular Probes) for 1 h in the dark and observed without washing. The CSLM imaging uses two visible-light lasers: (i) a 25-mW argon laser exciting at 458 nm (for calcofluor) and 488 nm (for GFP) and (ii) a 1-mW helium-neon laser exciting at 543 nm (for Alexa-concanavalin A). We used a 40× water immersion objective. Image analysis and three-dimensional reconstruction were conducted using Zeiss LSM5 Image browser software. Depth views are translucent images with an artificial color gradient indicating cells closest to (blue) and furthest from (red) the silicone.

RESULTS

Identification of biofilm-defective mutants. To identify genes required for biofilm development, we screened a set of *C. albicans* homozygous insertion mutants for biofilm forma-

TABLE 1. *C. albicans* strains

Strain	Genotype	Description	Reference or source
BWP17	*ura3*::λ*imm434*/*ura3*::λ*imm434* *arg4*::*hisG*/*arg4*::*hisG* *his1*::*hisG*/*his1*::*hisG*	Parent strain	54
DAY185	*ura3*::λ*imm434*/*ura3*::λ*imm434* *ARG4*:*URA3*::*arg4*::*hisG*/*arg4*::*hisG* *his1*::*hisG*::*pHIS1*/*his1*::*hisG*	Arg$^+$ Ura$^+$ His$^+$ reference strain	7
DAY286	*ura3*::λ*imm434*/*ura3*::λ*imm434* *ARG4*:*URA3*::*arg4*::*hisG*/*arg4*::*hisG* *his1*::*hisG*/*his1*::*hisG*	Arg$^+$ Ura$^+$ His$^-$ reference strain	8
GKO443	*ura3*::λ*imm434*/*ura3*::λ*imm434* *arg4*::*hisG*/*arg4*::*hisG* *his1*::*hisG*/*his1*::*hisG* *suv3*::Tn*7*-*UAU1*/*suv3*::Tn*7*-*URA3*	*suv3* GKO	8
GKO798	*ura3*::λ*imm434*/*ura3*::λ*imm434* *arg4*::*hisG*/*arg4*::*hisG* *his1*::*hisG*/*his1*::*hisG* *kem1*::Tn*7*-*UAU1*/*kem1*::Tn*7*-*URA3*	*kem1* GKO	8
GKO814	*ura3*::λ*imm434*/*ura3*::λ*imm434* *arg4*::*hisG*/*arg4*::*hisG* *his1*::*hisG*/*his1*::*hisG* *nup85*::Tn*7*-*UAU1*/*nup85*::Tn*7*-*URA3*	*nup85* GKO	8
GKO9	*ura3*::λ*imm434*/*ura3*::λ*imm434* *arg4*::*hisG*/*arg4*::*hisG* *his1*::*hisG*/*his1*::*hisG* *mds3*::Tn*7*-*UAU1*/*mds3*::Tn*7*-*URA3*	*mds3* GKO	8
MLR12	*ura3*::λ*imm434*/*ura3*::λ*imm434* *arg4*::*hisG*/*arg4*::*hisG* *his1*::*hisG*::*pHIS1*-*NUP85*/*his1*::*hisG* *nup85*::Tn*7*-*UAU1*/*nup85*::Tn*7*-*URA3*	*NUP85* reconstituted strain	This study
MLR28	*ura3*::λ*imm434*/*ura3*::λ*imm434* *arg4*::*hisG*/*arg4*::*hisG* *his1*::*hisG*/*his1*::*hisG* *kem1*::Tn*7*-*UAU1*::*pHIS1*-*KEM1*/*kem1*::Tn*7*-*URA3*	*KEM1* reconstituted strain	This study
MLR3	*ura3*::λ*imm434*/*ura3*::λ*imm434* *arg4*::*hisG*/*arg4*::*hisG* *his1*::*hisG*::*pHIS1*-*SUV3*/*his1*::*hisG* *suv3*::Tn*7*-*UAU1*/*suv3*::Tn*7*-*URA3*	*SUV3* reconstituted strain	40
MLR56	*ura3*::λ*imm434*/*ura3*::λ*imm434* *arg4*::*hisG*/*arg4*::*hisG* *his1*::*hisG*::*pTEF1*-*GFP*/*his1*::*hisG* *suv3*::Tn*7*-*UAU1*/*suv3*::Tn*7*-*URA3*	*suv3* GKO tagged with GFP	This study
MLR57	*ura3*::λ*imm434*/*ura3*::λ*imm434* *arg4*::*hisG*/*arg4*::*hisG* *his1*::*hisG*::*pTEF1*-*GFP*/*his1*::*hisG* *kem1*::Tn*7*-*UAU1*/*kem1*::Tn*7*-*URA3*	*kem1* GKO tagged with GFP	This study
MLR59	*ura3*::λ*imm434*/*ura3*::λ*imm434* *arg4*::*hisG*/*arg4*::*hisG* *his1*::*hisG*::*pTEF1*-*GFP*/*his1*::*hisG* *nup85*::Tn*7*-*UAU1*/*nup85*::Tn*7*-*URA3*	*nup85* GKO tagged with GFP	This study
MLR61	*ura3*::λ*imm434*/*ura3*::λ*imm434* *arg4*::*hisG*/*arg4*::*hisG* *his1*::*hisG*::*pTEF1*-*GFP*/*his1*::*hisG* *mds3*::Tn*7*-*UAU1*/*mds3*::Tn*7*-*URA3*	*mds3* GKO tagged with GFP	This study
MLR74	*ura3*::λ*imm434*/*ura3*::λ*imm434* *arg4*::*hisG*/*arg4*::*hisG* *his1*::*hisG*/*his1*::*hisG* *kem1*Δ::*ARG4*/*kem1*Δ::*URA3*	*kem1* deletion mutant	This study
MLR91	*ura3*::λ*imm434*/*ura3*::λ*imm434* *arg4*::*hisG*/*arg4*::*hisG* *his1*::*hisG*::*pHIS1*-*TEF1*/*his1*::*hisG* *kem1*Δ::*ARG4*/*kem1*Δ::*URA3*	His$^+$ *kem1* deletion mutant	This study
VIC21	*ura3*::λ*imm434*/*ura3*::λ*imm434* *arg4*::*hisG*/*arg4*::*hisG* *his1*::*hisG*/*his1*::*hisG* *mds3*::Tn*7*-*UAU1*::*pHIS1*-*MDS3*/*mds3*::Tn*7*-*URA3*	*MDS3* reconstituted strain	8

tion ability on slices of silicone catheter material. Screening was accomplished by visual inspection of silicone slices in 12-well plates after 60 h of culture. The wild-type reference strain and most insertion mutants formed a thick biofilm that made the silicone slice appear opaque (Fig. 1A) compared to the translucent appearance of an uninoculated control (Fig. 1C). Growth was mainly restricted to the silicone surface; removal of the silicone slice revealed medium with little turbidity, though some biofilm fragments were dislodged (Fig. 1D). We identified biofilm-defective strains that met four criteria. First, they caused a less opaque appearance of the silicone surface than the reference strain (Fig. 1B). Second, they caused substantial turbidity of the growth medium (Fig. 1E) and grew as rapidly as the reference strain in planktonic culture conditions (Table 2). Third, biofilm formation defects were evident for at least two independently created insertion mutants for each gene. Fourth, reconstitution of a wild-type allele for each insertion-bearing gene restored a biofilm formation ability comparable to that of the reference strain (see below). Insertions associated with a defect in biofilm formation lay in four genes: *SUV3*, *NUP85*, *MDS3*, and *KEM1*.

There is no single unifying theme among the functions of these genes, as inferred from studies of their *Saccharomyces cerevisiae* homologs. ScSuv3p is a mitochondrial RNA helicase that is required for respiratory competence (37). It has been recently reported that *C. albicans suv3* insertion mutants are also defective in chlamydospore formation (40). ScNup85p is a component of the Nup84 nuclear pore complex that is required

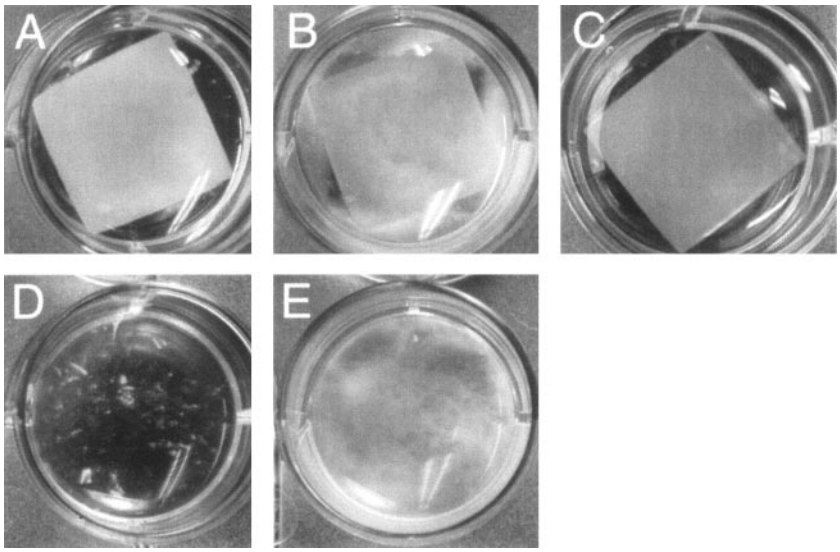

FIG. 1. Screen for biofilm-defective mutants. Squares from silicone sheets were inoculated and incubated for 60 h at 37°C in SD medium plus 50 mM glucose in wells of a 12-well plate. The wells are shown for (A) a typical nondefective insertion mutant, (B) a *kem1*/*kem1* insertion mutant, and (C) an uninoculated control. Growth of nonadherent cells was visualized after removal of the silicone squares for (D) the nondefective insertion mutant and (E) the *kem1*/*kem1* insertion mutant.

for poly(A) plus RNA export to the cytoplasm (13). Mds3p functions in *C. albicans* and *S. cerevisiae* to promote responses to alkaline growth conditions (8). In that context, we note that Rim101p, which functions independently of Mds3p to promote alkaline pH responses (8), is not required for biofilm formation (data not shown). ScKem1p, which has exoribonuclease activity, has pleiotropic roles in growth, mRNA turnover, nuclear fusion during mating, and filamentation (21, 23, 25, 26). Given that we identified 4 genes from among the 197 represented by this mutant collection and that there are approximately 5,600 nonessential genes in the *C. albicans* genome (80% nonessential gene fraction multiplied by 7,000 total genes [24]), we estimate that there are roughly 114 genes required for *C. albicans* biofilm formation.

The biofilm defect was quantified by measurement of the biomass dry weight retrieved from the silicone after 60 h of culture (Table 2). The mutants showed a dramatic reduction of biofilm mass. These findings argue that the mutants are capable of adherence to the silicone surface to produce a rudimentary biofilm but are defective in the production of a mature biofilm.

CSLM analysis. We used CSLM imaging in order to visualize the morphologies and structural organizations of the aberrant biofilms produced by the insertion mutants. The biofilms were grown under our standard conditions (in SD medium plus 50 mM glucose or in Spider medium, 37°, 60 h) and stained with calcofluor white concanavalin A, and reconstructed images were compared to those from the reference strain DAY185 and from reconstituted strains. The reference-strain biofilm (Fig. 2A and B) conforms to previously published biofilm descriptions (4, 17, 44). The basal layer, comprising primarily yeast cells, is poorly visible in these images because dye is excluded, presumably by the extracellular matrix and high cell density. (The basal yeast layer is discernible in image sections taken 4 μm and 10 μm above the silicone surface [Fig. 3A and B]). Above the poorly stained layer is a meshwork of pseudohyphae and hyphae, with a few long hyphae extending 150 μm to 250 μm away from the silicone surface (Fig. 2B).

One group of mutants, comprising the *suv3*/*suv3*, *nup85*/*nup85*, and *mds3*/*mds3* strains, is blocked at an early step of biofilm formation before any production of hyphae. These mutants form a thin 10-μm layer of cells (Fig. 2D, H, and M). The layer consists primarily of yeast cells, though a few elongated cells representing pseudohyphae are occasionally visible (Fig. 2C, G, and L). Reconstituted strains, in which a wild-type allele of each gene was restored, produced thick biofilms containing hyphae and excluded calcofluor from the basal cell layers (Fig. 2E, F, J, K, N, and O). Variation in biofilm depth of the reconstituted strains was similar to the day-to-day variation observed for reference strains.

TABLE 2. Growth of mutant strains in planktonic and biofilm states

Parameter	Results for[a]				
	DAY286 (reference strain)	GKO9 (*mds3*/*mds3*)	GKO443 (*suv3*/*suv3*)	GKO814 (*nup85*/*nup85*)	GKO798 (*kem1*/*kem1*)
Planktonic doubling time (min)	70 ± 1	71 ± 2	72 ± 0.5	88 ± 1	74 ± 0.5
Planktonic final OD_{600} after 25 h	3.5	4.5	2	5	4
Biofilm biomass (g [10^{-5}])	106 ± 30	6 ± 15	8 ± 9	6 ± 15	19 ± 9

[a] Planktonic doubling time and biofilm biomass results are expressed as means ± standard deviations.

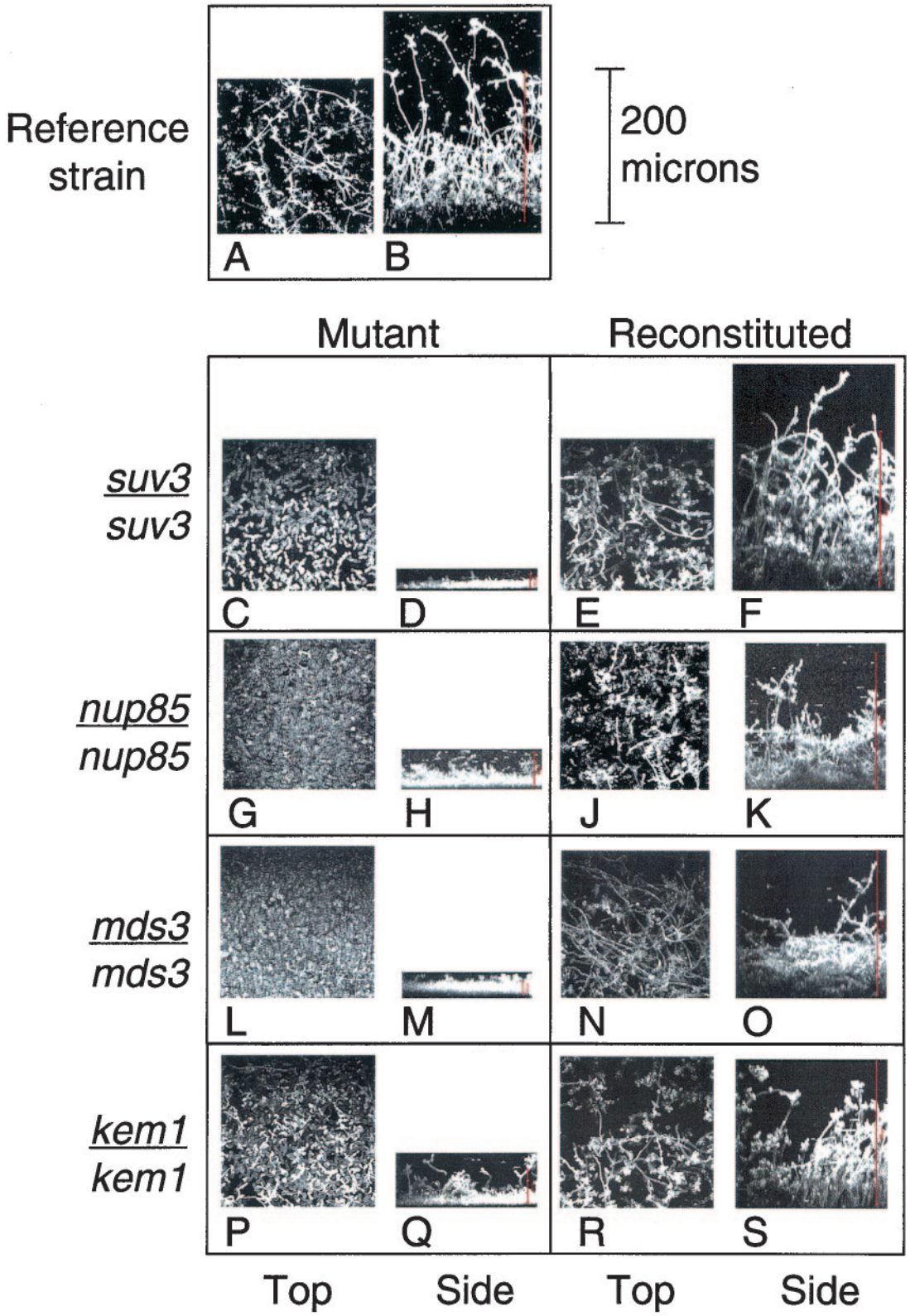

FIG. 2. CSLM images of biofilms stained with calcofluor white. Biofilms were cultured for 60 h at 37°C in SD medium plus 50 mM glucose and visualized with a 40× water immersion objective. Image reconstructions were created to provide views from above (*x-y* plane), which permit visualization of cell types (A, C, E, G, J, L, N, P, and R), and from the side (*z* plane; B, D, F, H, K, M, O, Q, and S), which permit visualization of depth. All images are presented at the same scale, and the silicone surface is at the bottom of each side view. Strains include the His^+ reference strain DAY185 (A and B), an *suv3*/*suv3* insertion mutant (C and D) and its *SUV3* reconstituted derivative (E and F), a *nup85*/*nup85* insertion mutant (G and H) and its *NUP85* reconstituted derivative (J and K), an *mds3*/*mds3* insertion mutant (L and M) and its *MDS3* reconstituted derivative (N and O), and a *kem1*/*kem1* insertion mutant (P and Q) and its *KEM1* reconstituted derivative (R and S). All of the insertion mutants were rendered His^+ through transformation with plasmid pGEM-HIS1 (7, 54) before cultivation for microscopy.

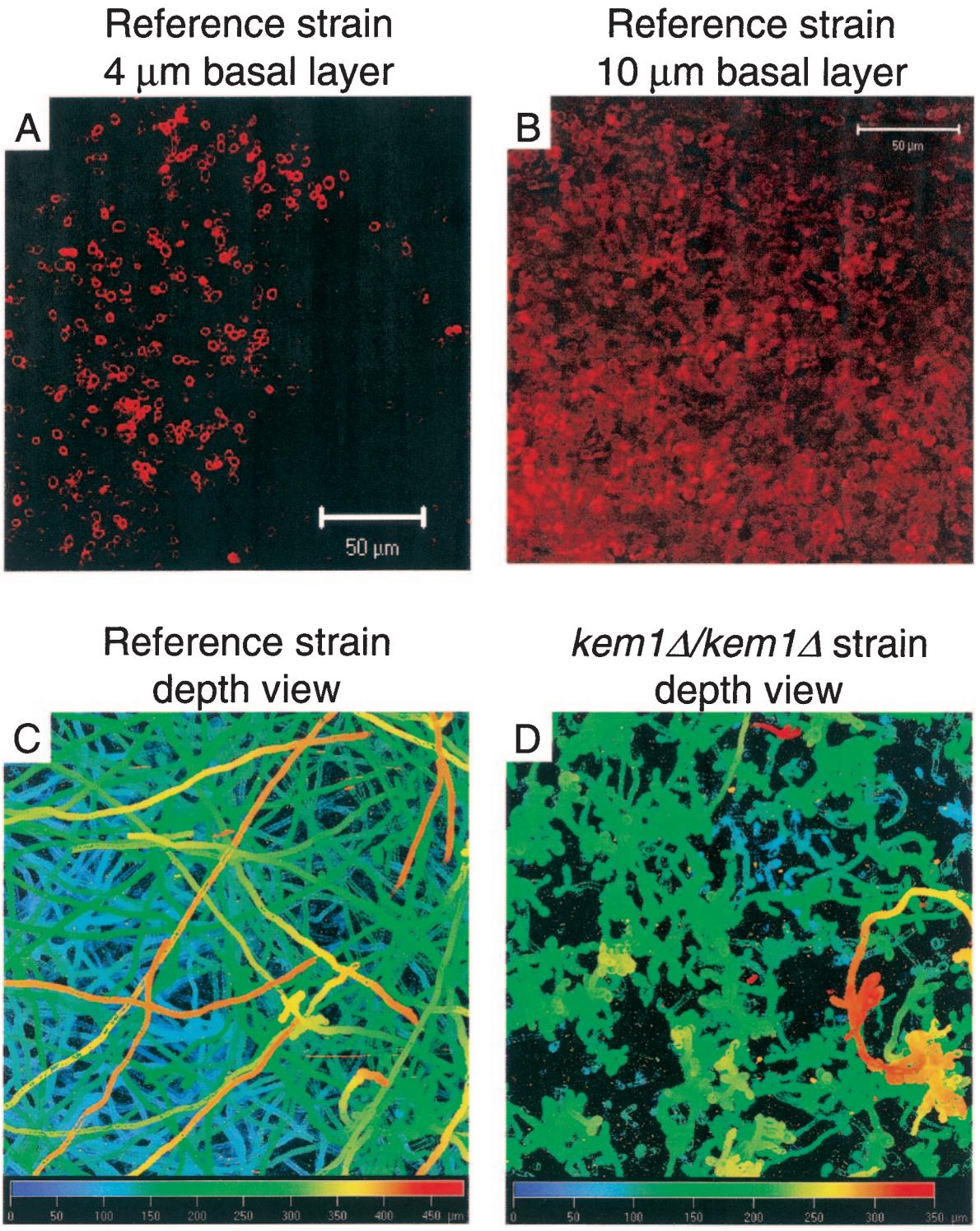

FIG. 3. CSLM images of biofilms stained with concanavalin A. Biofilms were cultured for 60 h at 37°C in Spider medium and visualized with a 40× water immersion objective, and images were reconstructed to yield views from above (*x-y* plane). (A and B) Single image slices of His^+ reference strain DAY185, taken 4 μm (A) or 10 μm (B) above the silicone surface, showing yeast cells populating the basal layer of the biofilm. (C and D) Image reconstructions were created to provide transparent depth views, with pseudocolor used to indicate depth of field, for (C) reference strain DAY185 and (D) *kem1*Δ/*kem1*Δ strain MLR91. Note that pseudocolor depth scales are slightly different for panels C and D.

The *kem1*/*kem1* mutant has a different phenotype than the other mutants, forming a 30-μm biofilm that includes yeast cells, pseudohyphae, and some rare hyphae (Fig. 2P and Q). Reconstitution of a *KEM1* allele restored the ability to form a normal biofilm (Fig. 2R and S), and a *kem1*Δ/*kem1*Δ strain lacking the entire *KEM1* ORF produced a 30-μm biofilm similar in appearance to the insertion mutant biofilm (data not shown). Therefore, a loss of Kem1p function causes a biofilm formation defect. The *kem1*/*kem1* insertion and deletion mutant strains both produced thick (~200-μm) biofilms in Spider medium that were similar in depth to reference-strain biofilms. However, examination of a CSLM depth view revealed a meshwork comprising almost exclusively long hyphae for the reference strain and primarily pseudohyphae for the *kem1*Δ/*kem1*Δ strain (Fig. 3C and D, respectively).

We conclude that there are two distinct phenotypic classes of mutants. In addition, restoration of biofilm formation ability in the reconstituted strains argues that the insertion mutations, rather than secondary mutations in the strains, cause the phenotypic defect in biofilm formation.

Hypha formation by biofilm-defective mutants. Hyphae are a prominent feature of biofilms. The mutants we identified appear to be partially or fully defective in hypha formation in the context of the biofilm. We considered two models for the proximal cause of the mutants' biofilm defects. One model is that the mutants have a general defect in hypha formation, and their failure to produce large adherent populations of cells on the substrate reflects a specific contribution of hyphae to adherence in the biofilm. A second model is that the mutants are defective in adherence, and their failure to produce hyphae is a consequence of diminished biofilm depth, so that no hypha-inducing signal is produced in the biofilm.

The first model would gain support if the mutants were defective in hypha formation under a variety of growth conditions; the second model would gain support if the mutants formed normal hyphae under these conditions. We reported previously that *mds3*/*mds3* mutants are defective in hypha formation in alkaline media, such as M199 medium, pH 8, and Spider medium (8). Indeed, all of the mutants failed to form abundant hyphae in M199 medium, pH 8 (Fig. 4) and Spider medium (data not shown). The *suv3*/*suv3*, *nup85*/*nup85*, and *kem1*/*kem1* mutants also failed to form hyphae in *N*-acetylglucosamine medium, while the *mds3*/*mds3* strain was competent to do so (data not shown). Reconstitution of wild-type alleles restored the ability to form hyphae (Fig. 4 and data not shown). All of the mutants formed hyphae in 5% serum (data not shown). These results indicate that these mutants are all defective in the formation of hyphae, at least under some conditions.

The two models make different predictions about the behavior of mutant cells in a mixed biofilm, comprising both wild-type and mutant cells. The first model predicts that the mutants will be unable to form hyphae in the context of a mixed biofilm, since hypha formation is their primary defect. The second model predicts that the mutants will form hyphae in a mixed biofilm, since their hypha formation defect is only a consequence of failure to produce an inducing signal. We observed that a 1:1 mixed inoculum of wild-type cells with each mutant formed a biofilm without producing appreciable turbidity of the culture medium, thus suggesting that mutant cells may be incorporated efficiently into the mixed biofilm. To determine whether the wild-type cells induced hyphal differentiation in cocultured mutants, we labeled each mutant strain through introduction of a *TEF1-GFP* reporter and monitored its growth in 1:1 wild-type:mutant mixed biofilms through confocal microscopy. For the *suv3*/*suv3* mutant, we observed the GFP signal primarily in the basal region of the biofilm (Fig. 5A), corresponding to the region excluding calcofluor (Fig. 5B). A few GFP-labeled cells were observed in the distal portions of the biofilm, and merging of the GFP and calcofluor images shows that these mutant cells are associated with GFP-negative hyphae (Fig. 5C). Very similar results were obtained with mixed biofilms of the wild type and either *mds3*/*mds3* or *nup85*/*nup85* mutants (data not shown); we only rarely observed GFP-labeled hyphae. We confirmed that GFP is detectable in hyphae of a wild-type strain carrying *TEF1-GFP* (data not shown). These results indicate that the mutants are defective in the production of hyphae in the context of a biofilm.

Mixed biofilms of the wild type and the *kem1*/*kem1* mutant (Fig. 5D through F) included some GFP-labeled filaments. Inspection of individual sections of the biofilm indicated that GFP-labeled filaments were primarily pseudohyphae, with constrictions between elongated cells (data not shown). This result indicates that the *kem1*/*kem1* mutant is capable of producing pseudohyphae in the context of a biofilm.

DISCUSSION

The architecture and development of *C. albicans* biofilms have been analyzed in considerable detail, but our understanding of biofilm genetic control is limited (9, 31). Here we have used a small collection of homozygous *C. albicans* insertion mutants to identify four genes that are required for normal biofilm development: *SUV3*, *MDS3*, *NUP85*, and *KEM1*. The genes represented among the insertion mutants were not chosen to represent specific functional classes, and we cannot relate the biochemical functions of these gene products to specific mechanisms that may be required for biofilm development. Despite this limitation, we can draw several conclusions about biofilm formation and biofilm regulatory genes that solidify our current understanding and help project a course for future analyses.

One conclusion from this study is that temporally defined stages of biofilm formation appear to be governed by distinct control mechanisms. The mutants blocked at the early biofilm stage have very similar phenotypes: their rudimentary biofilms have few filamentous cells, are about 10 μm thick, and do not exclude the dye from their basal layer. This observation suggests that matrix accumulation is dependent upon later events in biofilm development. The mutants are not simply growth arrested at the early temporal stage, because cells are released into the medium and planktonic growth rates are comparable to those of the reference strain. The *suv3*/*suv3* mutant saturates planktonic cultures at a twofold-lower density than the reference strain, a mild growth defect that does not account for its 10-fold reduction in biofilm biomass. Thus, we believe that the common biofilm phenotypic defects in these mutants may have a single molecular or cell biological origin.

Our assay for biofilm-induced hypha formation helps to define the origin of the mutants' defects. Our observations indi-

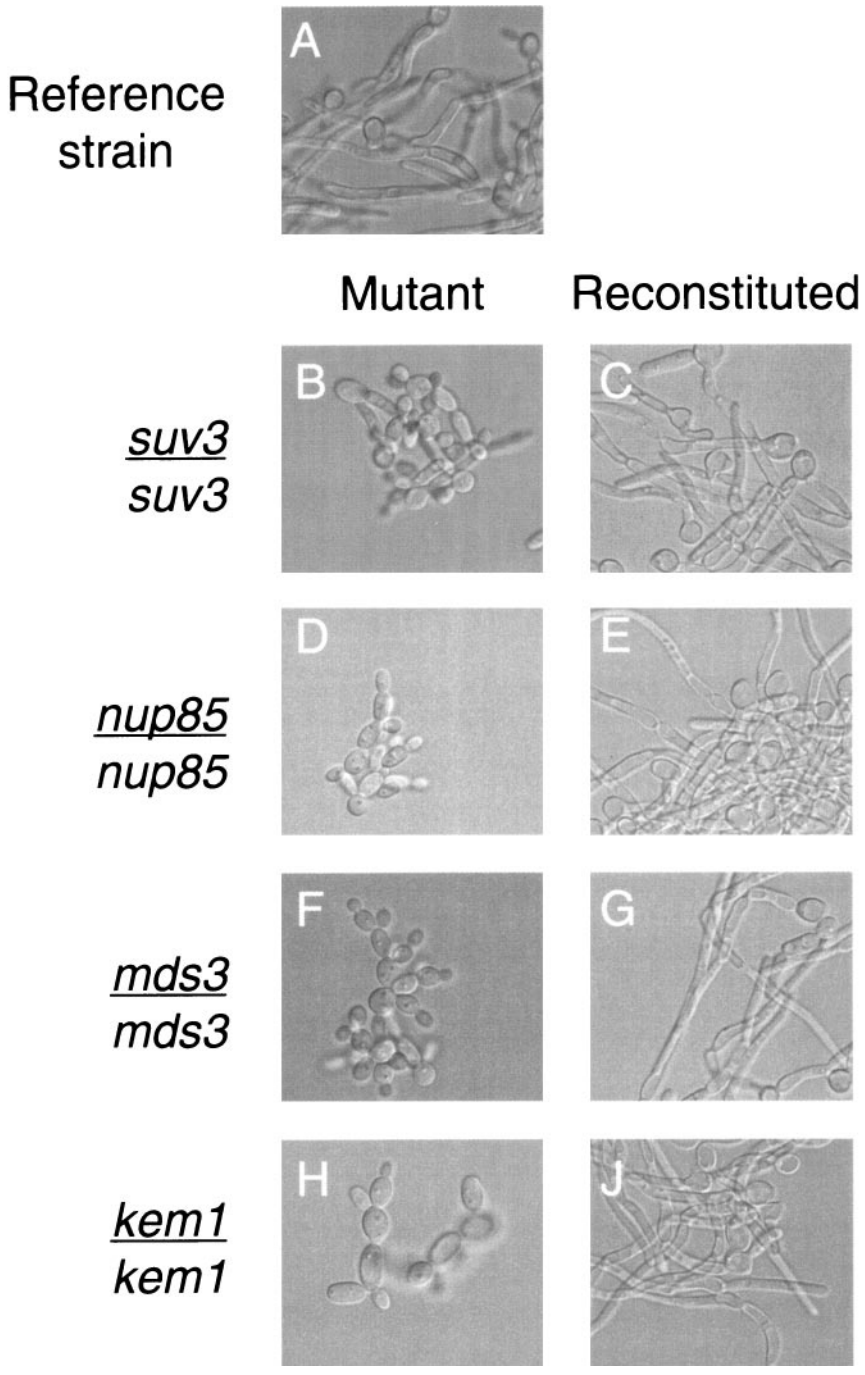

FIG. 4. Hypha formation assays of biofilm-defective mutants. Each strain was incubated in M199 medium, pH 8, at 37°C for 12 h. Culture samples were visualized at a ×400 magnification to visualize yeast cells and hyphae. All images are presented at the same magnification. Strains include the His^+ reference strain DAY185 (A), an *suv3*/*suv3* insertion mutant (B) and its *SUV3* reconstituted derivative (C), a *nup85*/*nup85* insertion mutant (D) and its *NUP85* reconstituted derivative (E), an *mds3*/*mds3* insertion mutant (F) and its *MDS3* reconstituted derivative (G), and a *kem1*/*kem1* insertion mutant (H) and its *KEM1* reconstituted derivative (J). All of the insertion mutants were rendered His^+ as described in the Fig. 2 legend.

cate that all of the mutants we have identified are defective in producing hyphae in the context of a biofilm, as they are during planktonic growth in several inducing media. Direct observation has shown clearly that hyphae are a component of *C. albicans* biofilms (9, 31), and it has been shown that hypha-defective mutants are defective in producing a substantial biofilm (1, 44). The use of the *efg1*/*efg1 cph1*/*cph1* mutant strain as a foundation for hyphal cause-effect arguments has been criticized because of uncertainty about the extent of its pleiotropy (28). Expression profiling experiments have lent credence to this argument, since the strain has altered expression of many cell wall protein genes along with several translation factors

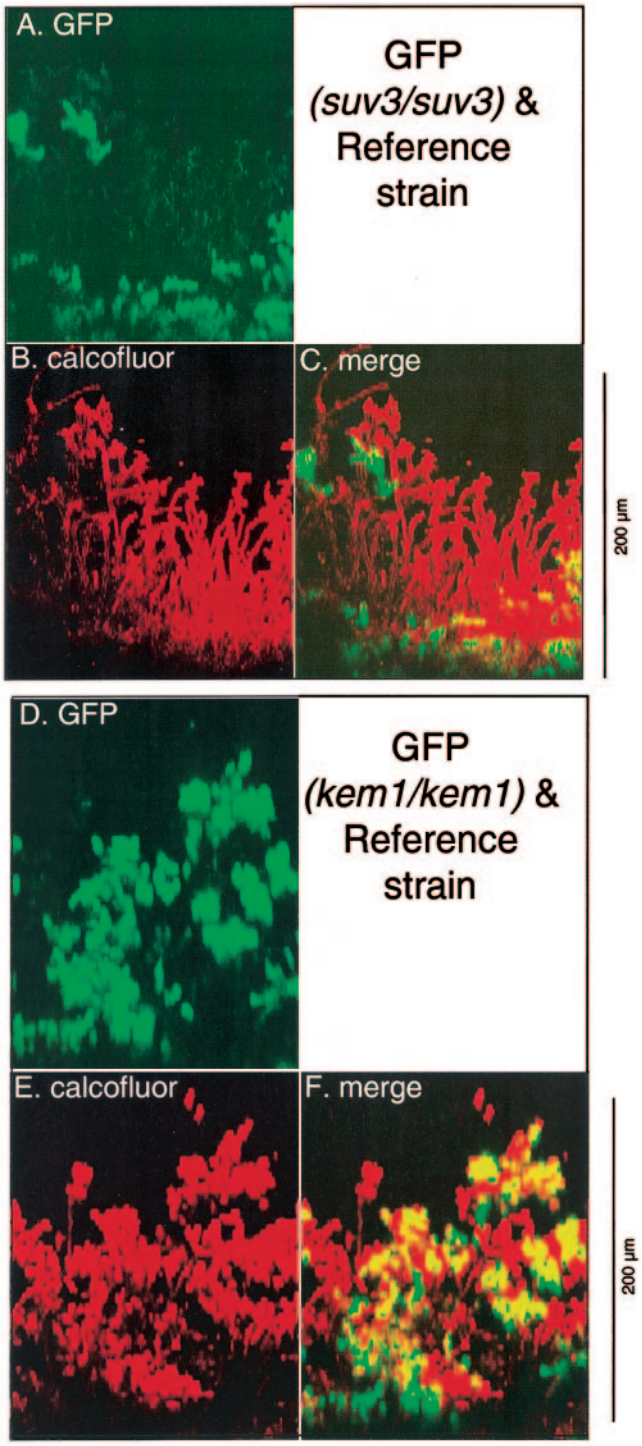

FIG. 5. Confocal images of mixed biofilms. Biofilms were cultured for 60 h at 37°C in SD medium plus 50 mM glucose and visualized with a 40× water immersion objective. The images are oriented with silicone at the bottom of each panel. Biofilms were created from a 1:1 inoculum of reference strain DAY185 with (A, B, and C) GFP-tagged *suv3*/*suv3* strain MLR56 or (D, E, and F) GFP-tagged *kem1*/*kem1* strain MLR57. Images show (A and D) GFP alone, (B and E) calcofluor alone, or (C and F) both GFP and calcofluor signals merged.

and transport modulators (39, 48). These gene expression changes may account for the altered adherence properties of *efg1*/*efg1 cph1*/*cph1* yeast cells when grown under biofilm-inducing conditions (11). Our *suv3*/*suv3*, *mds3*/*mds3*, and *nup85*/*nup85* mutants have more subtle hypha formation defects; for example, they produce hyphae in response to serum. Therefore, their biofilm-deficient phenotype strengthens the argument that mature biofilm formation depends upon hyphae, because these mutants clearly adhere to the silicone substrate and can populate the basal biofilm layer. Given that the mutants can be incorporated efficiently into mixed biofilms, we conclude that their adherence defect can be remedied by the presence of hyphae. Thus, we infer that the mutants' primary defect is in hypha formation and that the failure of mutant cells to adhere to their 10-μm biofilms is a consequence of the lack of hyphae.

If these mutants' biofilm defects arise from a hypha formation defect, it follows then that hyphae provide unique adherent surfaces that facilitate the formation of thick biofilms. This idea is in keeping with the increased expression of several *ALS* genes, which specify a surface adhesin family (19), in biofilms compared to planktonic cultures (4, 11, 15) and with the fact that several *ALS* genes are preferentially expressed during hyphal growth (10, 19, 20). The recent finding that adherence regulator Bcr1p is required for biofilm formation (40a) also supports this view.

The *kem1*/*kem1* mutant is clearly blocked at a different stage of biofilm formation than are the other mutants described here, based on the mass and depth of its rudimentary biofilm. In addition, its biofilms include substantial numbers of pseudohyphal cells, distinguishable by their elongated morphology and growth in filamentous chains. The extent of its biofilm defect is dependent on the medium, a feature commonly found among bacterial biofilm mutants (16, 41). However, *kem1*/*kem1* biofilms remain deficient in hyphae in both SD medium plus 50 mM glucose and Spider medium. The properties of the *kem1*/*kem1* mutant raise a type of question that is commonly encountered in analyses of developmental pathways. The question is whether the *kem1*/*kem1* terminal biofilm phenotype represents a true intermediate stage in normal biofilm development or whether it is an aberrant response to the primary mutant defect. The temporal analyses of Chandra et al. and of Hawser and Douglas did not reveal a stage in which only yeast cells and pseudohyphae were present (4, 17). In addition, we have not seen a distinct pseudohyphal layer in optical sections of biofilms. Thus, we believe that the preponderance of pseudohyphal cells produced by the *kem1*/*kem1* mutant does not reflect an intermediate stage in biofilm formation.

ACKNOWLEDGMENTS

We thank Theresa Swayne, Sudhindra Swamy, and Peter Carroll for their help with the use of the confocal microscope at the Columbia University Optical Microscopy Facility. We gratefully acknowledge the availability of the *C. albicans* genome sequence provided by the Stanford DNA Sequencing and Technology Center supported by the NIDR, NIH, and Burroughs Wellcome Fund, without which this work would not have been possible.

This work was supported by Public Health Services grants R01 AI50931, T32 AI07161 (V.M.B.), and T32 DK007786 (C.J.N.), for which we are very grateful. The Optical Microscopy Facility was es-

tablished by NIH Shared Instrumentation Grants S10 RR10506 and S10 RR13701 and by the Lieber Foundation. It is supported by NIH Grant P30 CA13696 as part of the Herbert Irving Comprehensive Cancer Center at Columbia University.

REFERENCES

1. **Baillie, G. S., and L. J. Douglas.** 1999. Role of dimorphism in the development of *Candida albicans* biofilms. J. Med. Microbiol. **48:**671–679.
2. **Bruno, V. M., and A. P. Mitchell.** 2004. Large-scale gene function analysis in *Candida albicans*. Trends Microbiol. **12:**157–161.
3. **Bruno, V. M., and A. P. Mitchell.** 2005. Regulation of azole drug susceptibility by *Candida albicans* protein kinase CK2. Mol. Microbiol. **56:**559–573.
4. **Chandra, J., D. M. Kuhn, P. K. Mukherjee, L. L. Hoyer, T. McCormick, and M. A. Ghannoum.** 2001. Biofilm formation by the fungal pathogen *Candida albicans*: development, architecture, and drug resistance. J. Bacteriol. **183:** 5385–5394.
5. **Cossart, P., and P. J. Sansonetti.** 2004. Bacterial invasion: the paradigms of enteroinvasive pathogens. Science **304:**242–248.
6. **Davey, M. E., and G. A. O'Toole.** 2000. Microbial biofilms: from ecology to molecular genetics. Microbiol. Mol. Biol. Rev. **64:**847–867.
7. **Davis, D., J. E. Edwards, Jr., A. P. Mitchell, and A. S. Ibrahim.** 2000. *Candida albicans RIM101* pH response pathway is required for host-pathogen interactions. Infect. Immun. **68:**5953–5959.
8. **Davis, D. A., V. M. Bruno, L. Loza, S. G. Filler, and A. P. Mitchell.** 2002. *Candida albicans* Mds3p, a conserved regulator of pH responses and virulence identified through insertional mutagenesis. Genetics **162:**1573–1581.
9. **Douglas, L. J.** 2003. *Candida* biofilms and their role in infection. Trends Microbiol. **11:**30–36.
10. **Fu, Y., A. S. Ibrahim, D. C. Sheppard, Y. C. Chen, S. W. French, J. E. Cutler, S. G. Filler, and J. E. Edwards, Jr.** 2002. *Candida albicans* Als1p: an adhesin that is a downstream effector of the EFG1 filamentation pathway. Mol. Microbiol. **44:**61–72.
11. **Garcia-Sanchez, S., S. Aubert, I. Iraqui, G. Janbon, J. M. Ghigo, and C. d'Enfert.** 2004. *Candida albicans* biofilms: a developmental state associated with specific and stable gene expression patterns. Eukaryot. Cell **3:**536–545.
12. **Gerami-Nejad, M., J. Berman, and C. A. Gale.** 2001. Cassettes for PCR-mediated construction of green, yellow, and cyan fluorescent protein fusions in *Candida albicans*. Yeast **18:**859–864.
13. **Goldstein, A. L., C. A. Snay, C. V. Heath, and C. N. Cole.** 1996. Pleiotropic nuclear defects associated with a conditional allele of the novel nucleoporin Rat9p/Nup85p. Mol. Biol. Cell **7:**917–934.
14. **Gow, N. A., A. J. Brown, and F. C. Odds.** 2002. Fungal morphogenesis and host invasion. Curr. Opin. Microbiol. **5:**366–371.
15. **Green, C. B., G. Cheng, J. Chandra, P. Mukherjee, M. A. Ghannoum, and L. L. Hoyer.** 2004. RT-PCR detection of *Candida albicans* ALS gene expression in the reconstituted human epithelium (RHE) model of oral candidiasis and in model biofilms. Microbiology **150:**267–275.
16. **Hall-Stoodley, L., J. W. Costerton, and P. Stoodley.** 2004. Bacterial biofilms: from the natural environment to infectious diseases. Nat. Rev. Microbiol. **2:**95–108.
17. **Hawser, S. P., and L. J. Douglas.** 1994. Biofilm formation by *Candida* species on the surface of catheter materials in vitro. Infect. Immun. **62:**915–921.
18. **Hawser, S. P., and L. J. Douglas.** 1995. Resistance of *Candida albicans* biofilms to antifungal agents in vitro. Antimicrob. Agents Chemother. **39:** 2128–2131.
19. **Hoyer, L. L.** 2001. The ALS gene family of *Candida albicans*. Trends Microbiol. **9:**176–180.
20. **Hoyer, L. L., T. L. Payne, M. Bell, A. M. Myers, and S. Scherer.** 1998. *Candida albicans* ALS3 and insights into the nature of the ALS gene family. Curr. Genet. **33:**451–459.
21. **Interthal, H., C. Bellocq, J. Bahler, V. I. Bashkirov, S. Edelstein, and W. D. Heyer.** 1995. A role of Sep1 (= Kem1, Xrn1) as a microtubule-associated protein in *Saccharomyces cerevisiae*. EMBO J. **14:**1057–1066.
22. **Jin, Y., H. K. Yip, Y. H. Samaranayake, J. Y. Yau, and L. P. Samaranayake.** 2003. Biofilm-forming ability of *Candida albicans* is unlikely to contribute to high levels of oral yeast carriage in cases of human immunodeficiency virus infection. J. Clin. Microbiol. **41:**2961–2967.
23. **Johnson, A. W.** 1997. Rat1p and Xrn1p are functionally interchangeable exoribonucleases that are restricted to and required in the nucleus and cytoplasm, respectively. Mol. Cell. Biol. **17:**6122–6130.
24. **Jones, T., N. A. Federspiel, H. Chibana, J. Dungan, S. Kalman, B. B. Magee, G. Newport, Y. R. Thorstenson, N. Agabian, P. T. Magee, R. W. Davis, and S. Scherer.** 2004. The diploid genome sequence of *Candida albicans*. Proc. Natl. Acad. Sci. USA **101:**7329–7334.
25. **Kim, J.** 2002. KEM1 is involved in filamentous growth of *Saccharomyces cerevisiae*. FEMS Microbiol. Lett. **216:**33–38.
26. **Kim, J., P. O. Ljungdahl, and G. R. Fink.** 1990. *kem* mutations affect nuclear fusion in *Saccharomyces cerevisiae*. Genetics **126:**799–812.
27. **Klemba, M., and D. E. Goldberg.** 2002. Biological roles of proteases in parasitic protozoa. Annu. Rev. Biochem. **71:**275–305.
28. **Kobayashi, S. D., and J. E. Cutler.** 1998. *Candida albicans* hyphal formation and virulence: is there a clearly defined role? Trends Microbiol. **6:**92–94.
29. **Kojic, E. M., and R. O. Darouiche.** 2004. *Candida* infections of medical devices. Clin. Microbiol. Rev. **17:**255–267.
30. **Kruppa, M., B. P. Krom, N. Chauhan, A. V. Bambach, R. L. Cihlar, and R. A. Calderone.** 2004. The two-component signal transduction protein Chk1p regulates quorum sensing in *Candida albicans*. Eukaryot. Cell **3:**1062–1065.
31. **Kumamoto, C. A.** 2002. *Candida* biofilms. Curr. Opin. Microbiol. **5:**608–611.
32. **Kumamoto, C. A.** 2005. A contact-activated kinase signals *Candida albicans* invasive growth and biofilm development. Proc. Natl. Acad. Sci. USA **102:** 5576–5581.
33. **Li, X., Z. Yan, and J. Xu.** 2003. Quantitative variation of biofilms among strains in natural populations of *Candida albicans*. Microbiology **149:**353–362.
34. **Liu, H.** 2001. Transcriptional control of dimorphism in *Candida albicans*. Curr. Opin. Microbiol. **4:**728–735.
35. **Liu, H., J. Kohler, and G. R. Fink.** 1994. Suppression of hyphal formation in *Candida albicans* by mutation of a STE12 homolog. Science **266:**1723–1726.
36. **Lo, H. J., J. R. Kohler, B. DiDomenico, D. Loebenberg, A. Cacciapuoti, and G. R. Fink.** 1997. Nonfilamentous *C. albicans* mutants are avirulent. Cell **90:**939–949.
37. **Minczuk, M., A. Dmochowska, M. Palczewska, and P. P. Stepien.** 2002. Overexpressed yeast mitochondrial putative RNA helicase Mss116 partially restores proper mtRNA metabolism in strains lacking the Suv3 mtRNA helicase. Yeast **19:**1285–1293.
38. **Naglik, J. R., S. J. Challacombe, and B. Hube.** 2003. *Candida albicans* secreted aspartyl proteinases in virulence and pathogenesis. Microbiol. Mol. Biol. Rev. **67:**400–428.
39. **Nantel, A., D. Dignard, C. Bachewich, D. Harcus, A. Marcil, A. P. Bouin, C. W. Sensen, H. Hogues, M. van het Hoog, P. Gordon, T. Rigby, F. Benoit, D. C. Tessier, D. Y. Thomas, and M. Whiteway.** 2002. Transcription profiling of *Candida albicans* cells undergoing the yeast-to-hyphal transition. Mol. Biol. Cell **13:**3452–3465.
40. **Nobile, C. J., V. M. Bruno, M. L. Richard, D. Davis, and A. P. Mitchell.** 2003. Genetic control of chlamydospore formation in *Candida albicans.* Microbiology **149:**3629–3637.

40a. **Nobile, C. J., and A. P. Mitchell.** 2005. Regulation of cell-surface genes and biofilm formation by the *C. albicans* transcription factor Bcr1p. Curr. Biol. **15:**1150–1155.

41. **O'Toole, G., H. B. Kaplan, and R. Kolter.** 2000. Biofilm formation as microbial development. Annu. Rev. Microbiol. **54:**49–79.
42. **Ramage, G., S. Bachmann, T. F. Patterson, B. L. Wickes, and J. L. Lopez-Ribot.** 2002. Investigation of multidrug efflux pumps in relation to fluconazole resistance in *Candida albicans* biofilms. J. Antimicrob. Chemother. **49:**973–980.
43. **Ramage, G., K. Vande Walle, B. L. Wickes, and J. L. Lopez-Ribot.** 2001. Standardized method for in vitro antifungal susceptibility testing of *Candida albicans* biofilms. Antimicrob. Agents Chemother. **45:**2475–2479.
44. **Ramage, G., K. VandeWalle, J. L. Lopez-Ribot, and B. L. Wickes.** 2002. The filamentation pathway controlled by the Efg1 regulator protein is required for normal biofilm formation and development in *Candida albicans*. FEMS Microbiol. Lett. **214:**95–100.
45. **Reagan, D. R., M. A. Pfaller, R. J. Hollis, and R. P. Wenzel.** 1990. Characterization of the sequence of colonization and nosocomial candidemia using DNA fingerprinting and a DNA probe. J. Clin. Microbiol. **28:**2733–2738.
46. **Riggle, P. J., K. A. Andrutis, X. Chen, S. R. Tzipori, and C. A. Kumamoto.** 1999. Invasive lesions containing filamentous forms produced by a *Candida albicans* mutant that is defective in filamentous growth in culture. Infect. Immun. **67:**3649–3652.
47. **Shin, J. H., S. J. Kee, M. G. Shin, S. H. Kim, D. H. Shin, S. K. Lee, S. P. Suh, and D. W. Ryang.** 2002. Biofilm production by isolates of *Candida* species recovered from nonneutropenic patients: comparison of bloodstream isolates with isolates from other sources. J. Clin. Microbiol. **40:**1244–1248.
48. **Sohn, K., C. Urban, H. Brunner, and S. Rupp.** 2003. EFG1 is a major regulator of cell wall dynamics in *Candida albicans* as revealed by DNA microarrays. Mol. Microbiol. **47:**89–102.
49. **Spreghini, E., D. A. Davis, R. Subaran, M. Kim, and A. P. Mitchell.** 2003. Roles of *Candida albicans* Dfg5p and Dcw1p cell surface proteins in growth and hypha formation. Eukaryot. Cell **2:**746–755.
50. **Stoodley, P., K. Sauer, D. G. Davies, and J. W. Costerton.** 2002. Biofilms as complex differentiated communities. Annu. Rev. Microbiol. **56:**187–209.
51. **Tripathi, G., C. Wiltshire, S. Macaskill, H. Tournu, S. Budge, and A. J. Brown.** 2002. Gcn4 co-ordinates morphogenetic and metabolic responses to amino acid starvation in *Candida albicans*. EMBO J. **21:**5448–5456.
52. **Tucker, S. L., and N. J. Talbot.** 2001. Surface attachment and pre-penetration stage development by plant pathogenic fungi. Annu. Rev. Phytopathol. **39:**385–417.
53. **Voss, A., R. J. Hollis, M. A. Pfaller, R. P. Wenzel, and B. N. Doebbeling.** 1994. Investigation of the sequence of colonization and candidemia in nonneutropenic patients. J. Clin. Microbiol. **32:**975–980.
54. **Wilson, R. B., D. Davis, and A. P. Mitchell.** 1999. Rapid hypothesis testing with *Candida albicans* through gene disruption with short homology regions. J. Bacteriol. **181:**1868–1874.